# Smart Electricity Meter Reliability Prediction based on Accelerated Degradation Testing and Modeling

Zhou Yang, Xun-Xia Chen, Yan-Fu Li, Enrico Zio, Rui Kang

# Smart Electricity Meter Reliability Prediction based on Accelerated Degradation Testing and Modeling

Z. Yang[1], Y. X. Chen[1], Y.F. Li[2], E. Zio[2,3], R. Kang[1]

[1]*Department of Reliability and System Engineering, Beihang University, China*

[2]*Chair on Systems Science and the Energetic Challenge, European Foundation for New Energy-Electricite' de France, at Ecole Centrale Paris- Supelec, France*

[3]*Politecnico di Milano, Italy*

**Abstract**: The smart electricity meter (SEM) is one of the most critical elements of smart grids. The billing function of SEM is one of its most important functions to its operators and end-users. Because the SEM devices need to be highly reliable, in this study we conduct accelerated degradation tests (ADTs) for the prediction of SEM reliability with respect to the billing function. For designing the ADTs, we have identified five key modules and their components, two performance indicators, and three possible degradation stressors. Six ADTs are conducted under different configurations of the stressors. The test data are then used to fit degradation paths by linear regression models. Extrapolation to the failure threshold allows the prediction of the Time-to-Failure of SEM. Finally, the reliable lifetime of the SEM is predicted by an accelerated degradation function which is obtained by fitting a Weibull failure time distribution.

***Key word: smart electricity meter, accelerated degradation test, reliable lifetime prediction***

## I. INTRODUCTION

A subject of interest today is the evolution of the networks for electrical energy supply and their conception/renovation as "smart" grids [1] with distributed generation, as opposed to the centralized power generation structure of the existing electric power grids. The concepts and configurations of smart grids vary sensibly with respect to the implementation at the different levels of the electrical infrastructure, i.e. the transmission and distribution systems (the level of the individual customer, and the related pricing issues, lie beyond the scope of the study presented in this paper). The smart grid is an auto-balancing, self-monitoring power grid that has the ability to sense when a part of its system is overloaded and reroute power to reduce

the overload and prevent a potential outage situation [2, 3, 4]. It is expected to improve the major weak points of the current electricity grid, by improving the communication and control functions [5-8]. This requires an effective, reliable and real-time information flow [9, 10] to be implemented through an advanced metering infrastructure (AMI) in which smart electricity meters (SEMs) are the communication and metering terminals for the purposes of billing and controlling by the distribution company (Figure 1) [11].

Figure 1 The structure of smart grid`s functions and its relationship with the SEM [11]

The SEM is an advanced meter that measures the consumption in more details than a conventional meter and optionally, but generally, transmits the information back to the local distribution system for monitoring and billing purposes [12]. It also allows to interact with the meter itself for controlling its functionalities, such as Time-of-Use prices (TOU) [13]. Many countries (e.g. France, Germany, United Kingdom, United States, etc.) had/have plans of intensive investments for replacing conventional meters with SEMs [14], and thus the reliability of SEM becomes a crucial issue for the service warranty and maintenance of the whole grid system [15, 16].

The reliability of electronic devices like SEM can be in general evaluated by empirical methods such as 217 Plus [17], Bellcore SR-332 [18], and IEC 62380 [19], which make use of component failure data to estimate system failure rates [20]. Because of their ease-to-use character in practical engineering situations, they are supported and implemented by many companies for evaluating the reliability of SEM [21]. However, due to the complexity of the interactions among the SEM components and the lack of the related failure data, the results obtained by these methods may not be representative of the realistic conditions [22]. Another method for SEM reliability estimation is based on the IEC 62059 standard, which makes use of the results of accelerated life testing (ALT) [23]. However, the major issue encountered by IEC 62059 ALT during its implementation is that the recommendation for at least 5 failures in 30 samples is difficult to achieve because the cost constraints and experiment conditions are such that often no failure occurs.

In addition, with the rapid technological advancements of SEM, the reliability of SEM has been significantly improved, which implies that ALT might not be very applicable in terms of financial cost and testing time.

In this paper, a new method is proposed for predicting the reliability of SEM based on the results of accelerated degradation testing (ADT) [24]. ADT is an effective testing technique for dealing with highly reliable devices. Different from traditional ALT, ADT requires the performance degradation indicators to be defined and the relationship between the degradation and the failure to be specified [25, 26].

Based on ADT, we propose a 5-step framework for the reliable lifetime prediction of SEM: (1) perform ADT with 64 (or 56) SEM samples tested under each of 6 different configurations of 3 testing stressors, normally temperature, humidity, and electricity at different levels; (2) fit linear regression models of the degradation paths using the data collected for the degradation indicators throughout the pre-defined testing time horizon; (3) predict the degradation to failure with respect to a performance threshold, and obtain the times to failure of the samples; (4) build an accelerated degradation function of the stressors by fitting a Time-to-Failure Weibull distribution whose scale parameter is substituted by the accelerated degradation function itself; (5) Evaluate the lower bound reliable lifetime of SEM using the Weibull distribution obtained in step 4.

Figure 2 5-step framework for the reliable lifetime prediction

The rest of the paper is organized as follows: Section II introduces the functional modules of SEM, the physical degradation process of SEM and the relevant influential stressors; Section III describes the ADT experiment setting, procedures and results; Section IV establishes the degradation model; Section V fits the Time-to-Failure Weibull model and uses it for reliability prediction; Section VI concludes this work.

## II. FUNCTIONALITY AND PHYSICAL DEGRADATION OF THE SEM

### A. *Functionality analysis of SEM*

From the functionality point of view, SEM is divided into the following 8 modules: communication module, indicating module, power supplying module, controlling module, encrypting module, billing module, metering module and timing module. Table I lists these modules and their functions.

TABLE I SEM MODULES AND THEIR FUNCTIONS

The system diagram of SEM functionality, as performed by the modules listed in Table I, is shown in Figure 3. Within the methodological work proposed in the paper, the reasons that we consider specifically the billing function to exemplify our reliability analysis procedure are: 1) it is the function most concerned by the operators and end-users, as it is directly related to the amount of payment; 2) it is indicated as one of the key functions defined by the reference standard [23].

During the billing function, the metering module acquires and measures the consumer's power consumption. Note that to have a clearly defined higher level structure of the SEM, in this study we regard all the components related to metering functionally as parts of the metering module. For example, a typical SEM contains a current sampling sub-module and a voltage sampling sub-module acquiring current and voltage data, respectively. The data collected by them are, then, sent to the metering microchip for signal filtering and A/D. All of the above mentioned components belong to metering module. The controlling module receives the measurements and transfers them to the billing module. The billing module computes the fee dependent on the referenced time received from the timing module and the power consumption measurements received from the controlling module. The power supplying module supplies the operating power to all the modules. The indicating module monitors the situations of running SEM and shows the needing information of electricity consumption by a LCD screen. The five modules, timing module, billing module, controlling module, metering module and power supplying module, are strongly related to the billing function.

Figure 3 The functional diagram of SEM

### B. *Physical degradation*

According to the practical requirements, SEM's performance is expected to be evaluated with respect to a number of performance indicators, which reflect different aspects of the operation and functional conditions of SEM. As mentioned in Section 2.A our interest is on the billing function of SEM, so we retain only the performance indicators relevant to such function. However, there appears to be no physical indicator to measure the correctness of the billing function directly. Among all measurable quantities, the power consumption and the timing are the most critical to the billing function. Therefore we have selected the indicators of basic errors (BE) and chronometer errors (CE) to measure these two quantities, and define them in accordance to the parameters of State Grid Corporation of China [27].

BE measures the deviation of the power consumption from a reference value and is defined as follows:

$$\mathrm{BE} = \frac{\mathrm{P_{ref}} - \mathrm{P_{test}}}{\mathrm{P_{ref}}} \times 100\% \quad (1)$$

where $\mathrm{P_{ref}}$ is the reference power consumptions indicating the initial value of a single SEM before the test, and the $\mathrm{P_{test}}$ is the testing power consumptions indicating the value of one observation during the test.

CE measures the deviation of the testing frequency from a reference value:

$$\mathrm{CE} = \frac{1}{\mathrm{H_{ref}} - \mathrm{H_{test}}} \quad (2)$$

where $H_{ref}$ is the reference clock frequency related to the chronometer of a SEM, and $H_{test}$ is one testing clock frequency value during the test.

The performance indicators are usually linked to specific failure modes, classified into different levels of criticality. For example, the IEC 62059 standard classifies the billing related failure modes into three criticality levels depending on the extent to which they affect the billing function: critical failure, major failure, minor failure (Table II). In our case we are concerned with the most critical failure class in Table II, with limiting thresholds of acceptable performance equal to $\pm 1.0\%$ and $\pm 0.5 s/day$ [22], respectively.

TABLE II BILLING-RELATED FAILURE MODES CLASSIFICATION OF IEC62059

### C. *Failure modes analysis: identification of failure modes and stressors*

In order to identify the possible degradation stressors, we decompose the relevant SEM modules into various components. Table III summarizes the decomposition and the possible stressors that can influence the performance of each component [18]. The identified stressors are the environmental stresses experienced by SEM under practical conditions.

TABLE III KEY COMPONENTS OF BILLING-RELATED MODULES AND THE STRESSORS [13]

The ways that the stressors affect BE and CE are presented as follows:

1) Temperature effects: The billing function, whose accuracy is measured by its BE, is carried out mainly by the metering and billing modules. The former processes the loading measurements by the diverter, and then transfers the measured signal to the metering chip. Due to the metallic material of the diverter, its resistance value is unstable when operating at high temperature, which in general results in decreased metering accuracy [28]. In addition, the stability of the reference value of the voltage of the metering chip is dependent on the proper operation of the power supplying module, whose components are not stable at a high temperature [29]. The chronometer error is used to measure the performance of the timing chip and the oscillator and both can be deterred by high temperature. The stability of the oscillator acts as the main factor affecting the stability of the timing function.
2) Humidity effects: Moisture enters the integrated chip (IC) via the gap of its package, possibly leading to failure [30]. Furthermore, moisture with high temperature can cause aging and oxidation of all components, which gradually deteriorate the performance of every module related to billing and time functions.

3) Electricity effects: The sampling circuit of SEM deals with large currents (above 10A), and thus generates significant amounts of heat inside the SEM. The high internal temperature can possibly lead to degradation/failure of the components, as discussed in item 1) above.

## III. ACCELERATED DEGRADATION TEST

### A. *Experiment setting and procedure*

#### *1) Experiment setting*

The experiment setting includes determining the number of testing samples, designing testing profiles, and deploying the testing system. The testing samples are from the two major SEM suppliers (Wasion and Sanxing) in the Chinese market. Their specifications are listed in Table IV. Because the specifications of the two types are identical, only one set is shown.

TABLE IV SPECIFICATIONS OF THE SEMS UNDER TEST

*Number of testing samples*

Consider $n$ identical and independent SEMs, each one with same reliability $R$ under the testing conditions. Let random variable $X$ denotes the number of failed SEM samples at the end of the testing. Then, the producer accepted failure risk $\alpha$ is defined as [31]:

$$\Pr\{X \leq x\} = \alpha \tag{3}$$

By the binomial distribution, $\alpha$ is computed as:

$$\sum_{i=0}^{x} \frac{n!}{i!(n-i)!}(1-R)^i R^{n-i} = \alpha \tag{4}$$

To determine $n$ for the test, we consider $x = \{0, 1\}$, $R = \{0.9, 0.95\}$ (for the requisite of highly reliable SEM), and the producer's confidence level $\gamma = 1 - \alpha = \{0.7, 0.8, 0.9\}$ (represent the lower bond, the acceptable and the ideal confidence levels, respectively). Consecutively assuming the producer is overconfident about the products, $n$ can be obtained by the following inequality:

$$\sum_{i=0}^{x} \frac{n!}{i!(n-i)!}(1-R)^i R^{n-i} \leq 1-\gamma \quad (5)$$

The solutions to *n* for each combination of the three parameters $x, R, \gamma$ are listed in Table IV.

TABLE V NUMBER OF SAMPLES *n* UNDER DIFFERENT SETTINGS

Considering one failure in testing (*x*=1), the confidence level $\gamma = 0.8$, and sample reliability $R = 0.95$, then the number of samples *n* should be ≥59 for each experiment run. This configuration is used because it can achieve the samples size of ideal confidence level. To provide redundant samples, the number of samples *n* actually tested has been set to 64. However, due to cost constraints, the samples for experiment run S6 (see Table V) are reduced to 56, which leads to a confidence level $\gamma_{56} = 0.78$ ($R = 0.95$).

*Testing Profile*

The normal operational temperature and electricity current for SEM range from -40°C to 60°C and 0A to 10A, respectively [27]. Under extreme testing conditions of high operational stresses, it is found that the failure threshold of temperature and electricity current for SEM are 120°C and 60A, respectively. On the contrary the highest working humidity (relative humidity (RH)) of SEM is not met during the testing, due to the capacity constraint of the testing chamber: the highest reachable temperature and humidity of the testing chamber are 80°C and 95%, respectively, but they cannot be achieved simultaneously, due to the capacity constraint of the testing chamber.

The lowest temperature, humidity and current levels are set to 55°C, 80%, and 20A, respectively. This is because: 1) the maximum nominal operating temperature of SEM is 60°C and ADT requires that the lowest testing temperature be close to the highest normal operating temperature in order to accelerate the aging of SEM; 2) it is found that BE and CE of SEM increase only when the RH is above 80%; 3) the changes of BE and CE are significant when the current level is above 20A. The three stressors have been divided into 2, and 3 levels, respectively.

Due to the cost constrains, the allowable number of ADT runs is 6. The six design points of our experiment are shown in Table V.

TABLE VI THE DESIGN OF THE SIX EXPERIMENT RUNS

Figure 4 shows that there are totally 18 possible design points considering all levels of the stressors. The star means unreached test design points due to the capability of the testing chamber; the polygon represents the adopted test design points; the dots are the rejected test design points, considering the actual degradation effectiveness of the stressors under these conditions.

Figure 4 Illustration of the design points

*Testing System*

The testing system consists of one testing chamber, one testing platform, one testing equipment and one connection wire. The testing platform with 64 SEMs installed is placed inside the chamber (Figure 5 (a)), while the testing equipment which provides the working power, controlling signal and reference current, is located outside of the chamber (Figure 5 (b)). They are connected by a low-resistance, high-temperature and humidity-tolerant wire installed by some of the authors. The testing equipment can be manipulated by one computer to emulate the operating situation of SEM (e.g. the 18 loading conditions of Table IV below) and collect the performance data.

Figure 5 SEM testing chamber, platform and equipment

2) Experiment procedure

At the pre-experiment stage, the initial values of the BE and CE are firstly obtained for each SEM undergoing testing. During one experiment cycle, the chamber first increases the levels of the stressors from the normal condition ($23^{o}$C, 45%RH, 10A) to one of the designed conditions in Table V, and then holds such conditions for 16 hours or 24 hours. After that, the chamber releases the stresses and returns them to normal condition. The test outputs (i.e. BE and CE) of each sample are recorded only after they are stable (8 hours period). During the stressing and releasing procedures, the samples do not work. The reason to repeat this increasing and decreasing procedure is to avoid vapor condensation in air, which may lead to unexpected failures of SEM.

Figure 6 Profile of one testing cycle

Due to the cost constraints, the censoring horizon is set to be 400 hours (online time). The online (i.e. accelerated) intervals are mainly 24 hours (Figure 6), and the offline (i.e. normal condition) testing interval is about 4 hours. In order to find the optimal size of the online interval, we have tried different intervals

ranging from 8 hours to 24 hours under the designs S4 and S6 which are the first two experiments performed, leading to 22 observations (including an initial testing). We have found 24-hour long online interval to be an optimal option, whose degradation effects and number of offline tests can meet the requirements of the experiment (Figure 7). The number of testing cycles for S2, S3 and S5 is 17 because of the total censoring horizon that has one 16-hour and sixteen 24-hour testing intervals. S1 has 15 cycles which include one 16-hour and fourteen 24-hour intervals due to a failure of the testing system. S4 and S6 have 22 cycles because the total online time 400 hours are split in five 8-hour, six 16-hour and eleven 24-hour intervals.

Figure 7 ADT profile

### *B. Results*

The CE degradation paths of one sample (No. 5000101) under different stress designs show a common increasing trend (Figure 8). It is noted that due to a failure of testing equipment, the censoring time of S1 is 328 hours instead of 400 hours. In order to build a realistic degradation model of SEM, we simulate the real operating condition [32] of SEM by considering all its 18 loading conditions (shown in Table VI below) during the offline testing. Figure 9 presents the degradation paths of the BE of the sample No. 5000101, which has the most significant degradation among all samples at design S2. It is shown that most of the 18 degradation paths exhibit the same trend. Figure 10 presents the degradation paths of BE of sample No. 5000101 at loading condition #2 under different stress designs.

Figure 8 Degradation path of CE of sample No. 5000101 under different designs

Figure 9 Degradation path of CE of all stresses conditions (sample NO. 5000101)

TABLE VII THE 18 DIFFERENT LOADS

Figure 10 Degradation curves of BE of loading condition No.2 at all stress designs (sample NO. 5000101)

## IV. DEGRADATION MODEL FITTING

Because BE and CE exhibit a monotonous trend in time and no failures are observed during the experiment horizon, we use the following linear regression model to extrapolate the degradation path beyond the horizon, up to failure

$$y = y_0 + \mu t + \varepsilon, \varepsilon \sim N(0, \sigma^2) \tag{6}$$

where $y$ is the testing results (BE and CE) measured at time $t$, $y_0$ is the pre-testing result, $\mu$ is the slope, and $\varepsilon$ is the noise following a normal distribution with mean equals to zero and variance $\sigma^2$.

Due to the assumption that the degradation paths are linear, we smooth the data by moving average #:

$$\hat{y}_i = \begin{cases} \frac{1}{2i-1}(y_1 + y_2 + \cdots + y_{2i-1}) & i < \frac{K+1}{2} \\ \frac{1}{K}\left(y_{i-\frac{K-1}{2}} + y_{i-\frac{K-1}{2}+1} + \cdots + y_{i+\frac{K-1}{2}}\right) & \frac{K+1}{2} \le i \le N_j - \frac{K+1}{2} \\ \frac{1}{2(N_j-i)+1}\left(y_{2i-N_j} + y_{2i-N_j+1} + \cdots + y_{N_j}\right) & N_j - \frac{K+1}{2} < i \le N_j \end{cases} \tag{7}$$

where $\hat{y}_i$ is the smoothed data point, $i$ is the time index of the data point being smoothed, $N_j (j = 1 \ldots 6)$ represents the total number of observations at every stress condition, and $K$ (an odd number) is the span size of the smoothing. $K$ is the parameter to be optimized for best smoothing. Two evaluation criteria, root mean square error (RMSE) and R-square, are used to measure the two aspects of the smoothing effect over each span of size $K$: deviation to the original data points and flatness, respectively. The former criterion is defined directly on the data as:

$$RMSE(K) = \sqrt{\frac{1}{N_j}\sum_{i=1}^{N_j}[y_i - \hat{y}_i]^2} \tag{8}$$

Instead, $R^2(K)$ is computed by fitting a linear regression model on the smoothed data points by:

$$R^2(K) = 1 - \frac{\sum_{i=1}^{n}(y_i - \hat{y}_i)^2}{\sum_{i=1}^{n}(y_i - \bar{y})^2} \tag{9}$$

where $\bar{y}$ is the mean value of the observations. As these two criteria are in general conflicting with each other, the weighted sum of them (after scaling into the same range [0, 1]) is used to guide the search for optimal $K$:

$$W(K) = 0.5 \times R^{2\prime}(K) - 0.5 \times RMSE'(K) \tag{10}$$

where $R^{2\prime}(K)$ and $RMSE'(K)$ are the scaled values. We assign equal weights 0.5 to each criterion, because accuracy and the flatness are equally important for our purposes. Figure 10 plots $W(K)$ against different $K$

values by using the data from sample No. 5000101 at design level S2. It is noted that 17 is the total number of data points collected during the testing at level S2, as it is the total number of testing cycles at level S2.

Figure 11 shows all 19 degradation paths (18 BE paths and 1 CE path) of the sample No. 5000101 at design level S2 after the smoothing operation.

Figure 11 The weighted value of SEM as span size increases (17 is the maximum span size in S2)

Figure 12 Degradation paths of the sample (No.5000101) after smoothing

Standard least-square regression is performed on each of the smoothed degradation paths. The results are summarized in Table VII.

TABLE VIII REGRESSION RESULTS OF THE SAMPLE NO.5000101 UNDER DESIGN LEVEL S2

## V. RELIABILITY MODEL

### A. *SEM Lifetime Prediction*

For each SEM at each design level, there are 19 competing regression functions that link the BEs and CE with the lifetime of the component. According to the standard of the Chinese State Grids company [27], the failure threshold of CE is

$$|\mathrm{CE}|_{max} = 0.5 \tag{11}$$

and the threshold of BEs is

$$|\mathrm{BE}|_{max} = 1 \tag{12}$$

Given the thresholds and the regression coefficients in Table VII, the predicted time $\hat{t}_i$ when degradation path *i* exceeds its corresponding threshold can be obtained by solving the regression equation in (6). We take $\hat{t} = \min(\hat{t}_1, \ldots, \hat{t}_{19})$ as the predicted lifetime of the whole SEM under a specific design level. Figure 13 shows the distribution of the predicted lifetimes of the SEMs cumulated under all the design levels.

Figure 13 Predicted lifetime of each sample at all stressed conditions

*B. Acceleration Model and Parameter Esitmation*

Based on [35], for more than two stressors the accelerated lifetime model of SEM has a general log-linear form:

$$t(\bar{X}) = e^{\alpha_0 + \sum_{j=1}^{m} \alpha_j X_j} \tag{13}$$

where $\alpha_j, (j = 0, \dots, m)$ are the parameters to be estimated and $\bar{X} = (X_j), (j = 1, \dots, m)$ is the vector of different stressors. In our case, $\bar{X} = \left(\frac{1}{T}, \frac{1}{RH}, \ln I\right)$ where $T$ is the absolute temperature, $RH$ (%) is relative humidity, and $I$ is the current.

*1) Three-parameter model*

The acceleration model considering all the stressors is defined in the following form [36]:

$$t = Aexp\left(\frac{B}{T}\right) exp\left(\frac{C}{RH}\right)(I^{-D}) \tag{14}$$

where $A$, $B$, $C$, $D$ are the parameters to be estimated. In (14) the three stressors are assumed to be independent from each other. The temperature and humidity follow a variation of the Eyring model of electronic devices [37], while the electricity follows the inverse power law model [36].

We considered four intensively used distributions of failure data modeling as our alternative choices namely Weilbull distribution, exponential distribution, normal distribution and log-normal distribution. The P-P plot (probability–probability plot) method was introduced to determine the best fitted one. The P-P plot is so constructed that if the theoretical distribution is adequate for the data, the graph of a function of t (y axis) versus a function of the sample cumulative distribution function (x axis) will be close to a straight line [35]. Compared with other distribution, the results illuminate that Weilbull distribution is relatively reasonable for our data (Figure 14).

So we estimate the parameters of Weibull distribution as follows,

$$t \sim Weibull\left(exp\left(\alpha_0 + \frac{\alpha_1}{T} + \frac{\alpha_2}{RH} + \alpha_3 \ln I\right), m\right) \tag{15}$$

where $\alpha_0 = \ln A, \alpha_1 = B, \alpha_2 = C, \alpha_3 = -D$.

Figure 14 Time-to-Failure data goodness-of-fit of the Weibull distribution

To estimate the parameters $\alpha_0, \alpha_1, \alpha_2, \alpha_3$ and $m$, we conduct the maximum likelihood estimation (MLE). The MLE function is:

$$L(\alpha_0, \alpha_1, \alpha_2, m) = \prod_{i=1}^{p} \prod_{j=1}^{q_i} \left\{ m t_{ij}^{m-1} exp\left[ -m\left( \alpha_0 + \frac{\alpha_1}{T} + \frac{\alpha_2}{RH} + \alpha_3 \ln I \right) \right] \right\} \times exp\left\{ -t_{ij}^{m-1} exp\left[ -m\left( \alpha_0 + \frac{\alpha_1}{T} + \frac{\alpha_2}{RH} + \alpha_3 \ln I \right) \right] \right\} \quad (16)$$

where $t_{ij}$ is the time to failure of the $j$th ($j$=1, 2, … $M$) sample under the $S_i$ ($i$=1, 2, … 6) stress level. By setting $\frac{\partial \ln L}{\partial \alpha_0} = 0, \frac{\partial \ln L}{\partial \alpha_1} = 0, \frac{\partial \ln L}{\partial \alpha_2} = 0, \frac{\partial \ln L}{\partial \alpha_3} = 0, \frac{\partial \ln L}{\partial m} = 0$, we can obtain the MLE $\hat{\alpha}_1, \hat{\alpha}_2, \hat{\alpha}_3, \hat{\alpha}_4, \hat{m}$. The results are shown in Table VIII.

TABLE IX PARAMETER ESTIMATES OF THE THREE-STRESSORS ACCELERATION MODEL

*2) Two-parameter model*

Based on the results of Table VIII, the parameter of current $\alpha_3 = 0.2251$ is negligible comparing to the coefficients of the other stressors. To confirm this observation, we conduct a Wilcoxon signed rank test [39] to compare the lifetime data of two paired groups: S1 vs. S2 and S5 vs. S6, because the temperature and humidity levels are the same within these two groups. Table IX summarizes the results and shows that there is no significant difference regarding the paired lifetimes within each group.

The reasons of the fact that the electricity has little impact onto SEM degradation are presented as follows: the power supply to the SEM and the electricity measured by the SEM are different. The electricity level is raised to amplify the condition which SEM measures, while the power supply is stable during the testing. Because the electricity acquiring circuit is isolated from the main operational SEM circuit, the electricity can only cause minor effects onto the rest of the SEM by generating small amounts of heat. However, the ambient temperature inside the testing chamber is controlled by the constant blow of heated air. The local heat generated by the electricity acquiring circuit is quickly removed away and therefore has little impact onto the degradation of the SEM.

TABLE X PREDICTED LIFETIME OF ALL THE SAMPLES AT TWO PAIRED DESIGN LEVELS

Therefore, the accelerated model is modified eliminating current:

$$t = Aexp\left(\frac{B}{T}\right) exp\left(\frac{C}{RH}\right) \tag{17}$$

The parameter estimates of the two-parameter acceleration model are calculated by the same procedure as the 3-parameters model and the results are shown in Table X.

TABLE XI PARAMETER ESTIMATION OF TWO-STRESSORS ACCELERATED MODEL

### C. *Reliable Lifetime Evaluation*

As shown in Section IV.B, the lifetime of SEM follows a Weibull distribution with parameters $\eta$ and m, and $\eta$ can be obtained from (16); so, the reliability function of SEM can be written as,

$$R = e^{-\left(\frac{t}{\eta}\right)^m} = e^{-\left(\frac{t}{\alpha_0+\frac{\alpha_1}{T}+\frac{\alpha_2}{RH}}\right)^m} \tag{18}$$

Taking the natural log twice on both sides of (17),

$$ln\, t = \alpha_0 + \frac{\alpha_1}{T} + \frac{\alpha_2}{RH} + \frac{1}{m} ln\, ln(\frac{1}{R}) \tag{19}$$

where $t$ is the reliable lifetime (the lifetime of a device given a predefined reliability level) [40]. For the Weibull distribution, the lower bound of the reliability lifetime $t_\gamma$ can be obtained by [40, 41]:

$$ln\, t_\gamma = lnt - u_\gamma\sqrt{Var(ln\, t)} \tag{20}$$

where the index $\gamma$ indicates the confidence levels and $Var(\ln t)$ is the variance of $\ln t$ [36]:

$$\begin{aligned} Var(\ln t) = {} & \frac{\partial^2 \ln t}{\partial^2 \alpha_0} Var(\alpha_0) + \frac{\partial^2 \ln t}{\partial^2 \alpha_1} Var(\alpha_1) + \frac{\partial^2 \ln t}{\partial^2 \alpha_2} Var(\alpha_2) + \frac{\partial^2 \ln t}{\partial^2 m} Var(m) \\ & + 2\frac{\partial^2 \ln t}{\partial \alpha_0 \partial \alpha_1} cov(\alpha_0, \alpha_1) + 2\frac{\partial^2 \ln t}{\partial \alpha_0 \partial \alpha_2} cov(\alpha_0, \alpha_2) + 2\frac{\partial^2 \ln t}{\partial \alpha_0 \partial m} cov(\alpha_0, m) \\ & + 2\frac{\partial^2 \ln t}{\partial \alpha_1 \partial \alpha_2} cov(\alpha_1, \alpha_2) + 2\frac{\partial^2 \ln t}{\partial \alpha_1 \partial m} cov(\alpha_1, m) + 2\frac{\partial^2 \ln t}{\partial \alpha_2 \partial m} cov(\alpha_2, m) \\ \equiv {} & Var(ln\, t) = \frac{2\, ln\, ln\, R^{-1}}{m^3} Var(m) \end{aligned} \tag{21}$$

Substituting the estimated parameters $m$, $\alpha_0$, $\alpha_1$ and $\alpha_2$ into (19) given the normal conditions (*I=10A, T=20 ℃* or *25 ℃, RH=45%*) of SEM operation, the lower bound of the reliable lifetime at different confidence levels and reliability values is calculated (Table XI).

TABLE XII Reliable lifetime $t_\gamma$ of SEM

## VI. CONCLUSIONS

Reliability of SEM plays an important role for an effective answer to the question of future electric grids. In order to estimate it, ALTs, based on IEC62059 or other standards, are often conducted. However in a situation of evaluation of more reliable products, ADT can be a more capable, flexible and practical option, such as SEM, which only need to trace the deterring indicators of products during the test.

The major difficult to apply ADT to SEMs is how to determine the performance indicators and the testing profile that monitored in tests. In this work, an example of performance indicators, which are BE and CE, is given by taking into account the major function, configuration and key components of SEM. Also, the failure mechanism both in inner component and functional output are considered. Based on that, the testing profile including numbers of samples, testing environment stress, testing profile and testing platform are then devised.

With respect to predict the reliability, in terms of reliable life, based on the degradation information, pseudo life method was introduced. The key to pseudo life method is how to capture the best fitting function of degradation path. In this respect, a linear regression with moving average is presented. To determine the optimal number of moving average span and RMSE, a discriminant is developed and used, as the result of which 17 is the best span number. Compared with several alternative distributions, Weilbull distribution can provide a better fitting solution of pseudo life.

Because we have applied temperature, humidity and current as three accelerated testing stress to test, we firstly assume that it should be a three-parameters degradation function, but the result indicates current should not be involved, which means it is a two-parameters degradation function. The reliable life of the SEMs is obtained by MLE of the Weibull distribution considering its parameters as ADT function.

The scope of future work is how to conduct a demonstration test based on the predicting results of ADT. A work of sample determining method has already been presented on account of this paper`s contribution [42].

## VII. ACKNOWLEDGEMENT

This research work is funded by the project entitled “Reliability of smart electricity meter”, which is supported by Center of Meteorology of North China Grid Company. Also authors want to thank all the reviewers who provide assistances to improve this paper.

## References:

[1] Heckel J. Smart substation and feeder automation for a smart distribution grid. In: Proc. CIRED 2009 - 20th Int. Conf. and Exhibition on Electr. Distrib., part 1, Jun. 8-11, 2009.

[2] Granger Morgan M, Apt J, Lave LB, Ilic MD, Sirbu M, Peha JM. The many meanings of Smart Grid. A Briefing Note from the Department of Engineering and Public Policy, Carnegie Mellon University, Jul. 2009 at < http://repository.cmu.edu/epp/22/>.

[3] Hajian-Hoseinabadi H. Reliability and component importance analysis of substation automation systems. International Journal of Electrical Power &Energy Systems, in press.

[4] Daemi T, Ebrahimi A, Fotuhi-Firuzabad M. Constructing the bayesian network for components reliability importance ranking in composite power systems. International Journal of Electrical Power & Energy Systems, 2012;43(1):474-480.

[5] Farhoodnea M, Mohamed A, Shareef H. Identification of multiple harmonic sources in power systems using independent component analysis and mutual information. International Journal of Engineering Intelligent Systems, 2010;18(1): 51--63.

[6]. Tan X, Li Q, Wang H. Advances and trends of energy storage technology in Microgrid. International Journal of Electrical Power & Energy Systems, 2013.;44(1):179-191.

[7]. Chang L, Wu Z. Performance and reliability of electrical power grids under cascading failures. International Journal of Electrical Power & Energy Systems, 2011;33(8):1410-1419.

[8] Smart Grid Laboratory - Energylab, Smart Grid. Le reti elettriche di domani. Milano, Italy: Gruppo Italia Energia (Gieedizioni), 2011 (in Italian).

[9] Arya, LD, Choube SC, Arya R. Probabilistic reliability indices evaluation of electrical distribution system accounting outage due to overloading and repair time omission. International Journal of Electrical Power & Energy Systems, 2011;33(2): 296-302.

[10] Sood VK, Fischer D, Eklund JM, Brown T. Developing a communication infrastructure for the Smart Grid. In: Proc. IEEE Electr. Power Energy Conf. (EPEC), Oct. 22 - 23, Montréal, Canada, IEEE, 2009.

[11] Ilić MD, Xie L, Khan UA, Moura JMF. Modeling of future cyber – physical energy systems for distributed sensing and control. IEEE Trans. Syst. Man Cybern. A, Syst. Humans 2010;40(4):825-38.

[12]. Ren P, Xiang Z, Qiu Z. Intelligent domestic electricity management system based on analog-distributed hierarchy. International Journal of Electrical Power & Energy Systems, 2013;46(0):400-404.

[13] Farhangi H. The path of the smart grid. IEEE Trans on Power and Energy 2010;8(1):18-28.

[14] Gungor VC, Sahin D, Kocak T, Ergut S, Buccella C, Cecati C, Hancke GP. Smart grid technologies: communication technologies and standards. IEEE Trans on Industrial Informatics 2011;7(4):529-39.

[15] Depuru SSSR, Wang LF, Devabhaktuni V. Smart meters for power grid: challenges, issues, advantages and status. Renewable and Sustainable Energy Reviews 2011;15(6):2736-42.

[16] Kalinowski B, Anders G. A new look at component maintenance practices and their effect on customer, station and system reliability. International Journal of Electrical Power & Energy Systems 2006;28(10):679-95.

[17] Reliability Prediction Procedure for Electronic Equipment. AMSC MIL-HDBK-217F;1991.

[18] Reliability prediction procedure for electronic equipment. Telcordia, Std. SR-332;2006.

[19] Reliability data handbook-universal model for reliability prediction of electronics components, PCBs and equipment. IEC Std. 62380;2004.

[20] Bowles JB. A survey of reliability-prediction procedures for microelectronic devices. IEEE Transactions on Reliability 1992;41(1):2-12.

[21] Jones J, Hayes J. A comparison of electronic-reliability prediction models. *Reliability*, IEEE Transactions on Reliability 1999;48(2):127-34.

[22] Cushing MJ, Mortin DE, Stadterman TJ, Malhotra A. Comparison of electronics-reliability assessment approaches. IEEE Transactions on Reliability 1993;42(4):542-46.

[23] Electricity metering equipment-dependability, part 31: temperature and humidity accelerated reliability testing. IEC Std. 62059-31;2008.

[24] Meeker WQ, Escobar LA, Lu CJ. Accelerated degradation tests: modeling and analysis. Technometrics 1998;40(2):89-99.

[25] Oliveira VRB, Colosimo EA. Comparison of methods to estimate the time-to-failure distribution in degradation tests. Quality and Reliability Engineering International 2004;20(4):363-73.

[26] Si XS, Wang WB, Hu CH, Zhou DH, Pecht MG. Remaining useful life estimation based on a nonlinear diffusion degradation process. IEEE Transactions on Reliability 2012;61(1):50-67.

[27] Smart electricity meter standards assembly. Chinese State Grid Co,. 2011;(in Chinese).

[28] Wondrak W. Physical limits and lifetime limitations of semiconductor devices at high temperatures. Microelectronics Reliability 1999.;39(6–7):1113-20.

[29] Lu H, Bailey C, Yin C. Design for reliability of power electronics modules. Microelectronics Reliability 2009;49(9–11): 1250-55.

[30] Roesch WJ. Historical review of compound semiconductor reliability. Microelectronics Reliability 2006;46(8):1218-127.

[31] Kolarik WJ. Creating quality: concepts, systems, strategies, and tools. McGraw-Hill College; 1995.

[32] Vournas CD, Sauer PW, Pai MA. Relationships between voltage and angle stability of power systems. International Journal of Electrical Power and Energy Systems 1996;18(8):493-00.

[33] Alessio E, Carbone A, Castelli G, Frappietro V. Second-order moving average and scaling of stochastic time series. The European Physical Journal B-Condensed 2002;27(2):197-00;

[34] Vandewalle N, Ausloos M. Crossing of two mobile averages: a method for measuring the roughness exponent. Phys. Rev. E 1998;58(5):6832-34.

[35] Nelson W. Accelerated testing: statistical models, test plans and data analyses. Wiley Online Library; 1990.

[36] Escobar LA. Meeker WQ. A review of accelerated test models. Statistical Science 2006;21(4):552--77.

[37] Striny K, Schelling A. Reliability evaluation of aluminum-metallized mos dynamic ram's in plastic packages in high humidity and temperature environments. IEEE Transactions on Components, Hybrids, and Manufacturing Technology 1981;4(4): 476-81.

[38] Littell RC, McClave JT, Offen WW. Goodness-of-fit tests for the two parameter Weibull distribution. Communications in Statistics - Simulation and Computation 1979;8(3):257-69.

[39] Walpole RE, Myers RH, Myers SL, Ye K. Probability and statistics for engineers and scientists. Saddle River, NJ: Prentice Hall Upper; 1998.

[40] Nelson W. Applied Life Data Analysis, New York: John Wiley & Sons, Inc., 1982.

[41] Kececioglu D, Gill RD, Keiding N, Hamilton LC. Reliability & Life Testing Handbook. Englewood Cliffs, NJ: Prentice Hall, Inc. Vol. 1 and 2, 1993 and 1994.

[42]. Hui Z, Qinfeng C, Hanji Ju, Xiaolei, Z, Single sampling inspection method of smart meter according to reliable life. Quality, Reliability, Risk, Maintenance, and Safety Engineering (ICQR2MSE), 2012 International Conference; 15-18 June 2012;829-832.

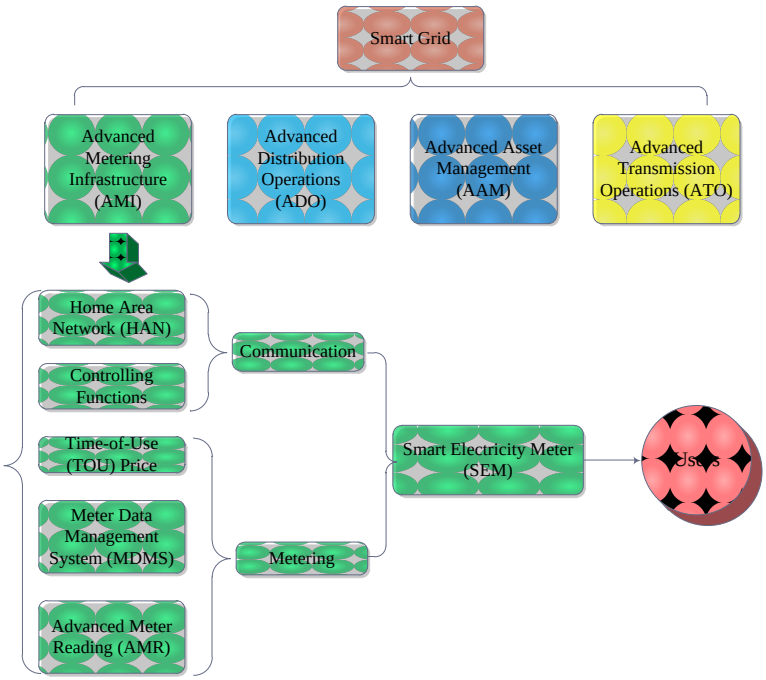


Figure 1. The structure of smart grid`s functions and its relationship with the SEM

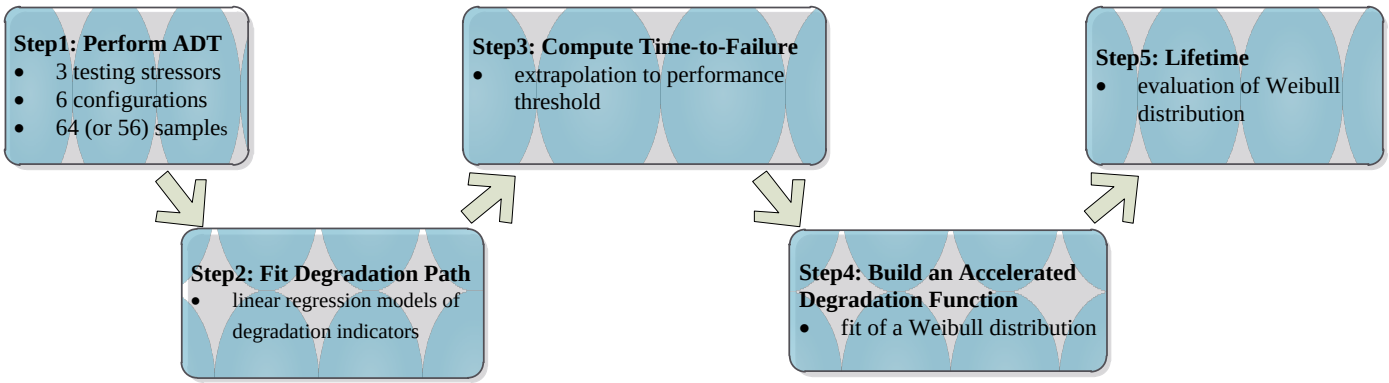

Figure 2. 5-step framework for the reliable lifetime prediction

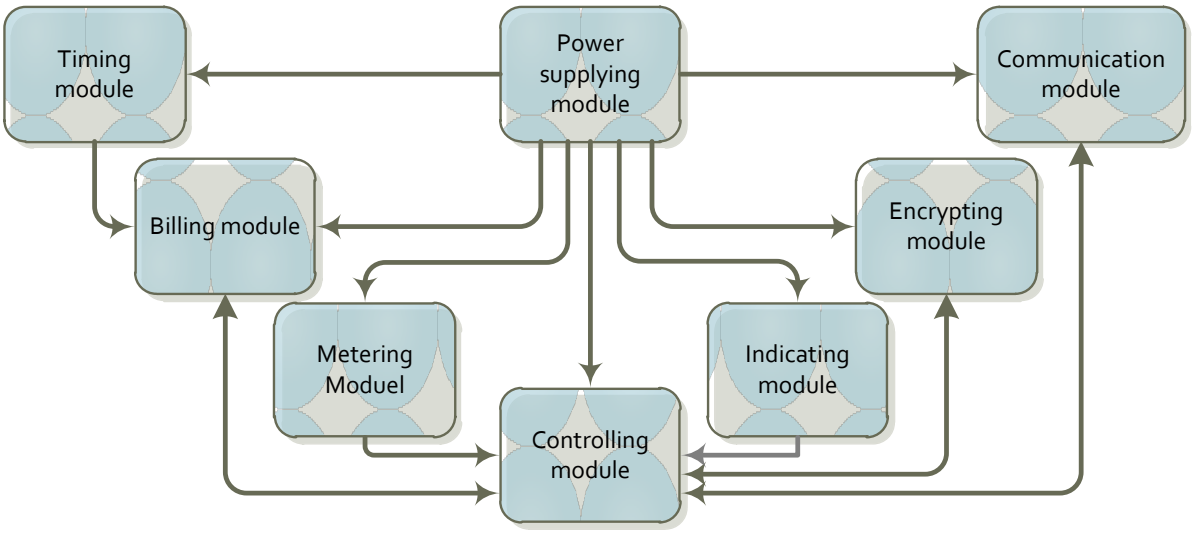


Figure 3. The functional diagram of SEM

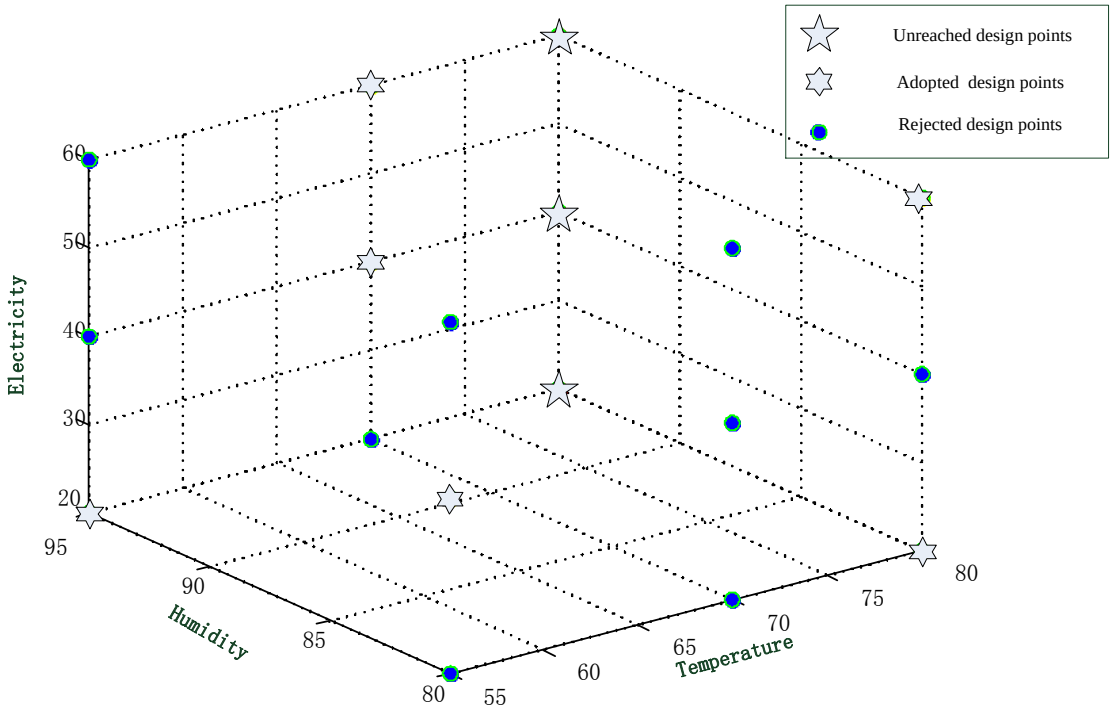


Figure 4. Illustration of the design points

(a) (b)

Figrure 5. SEM testing chamber, platform and equipment

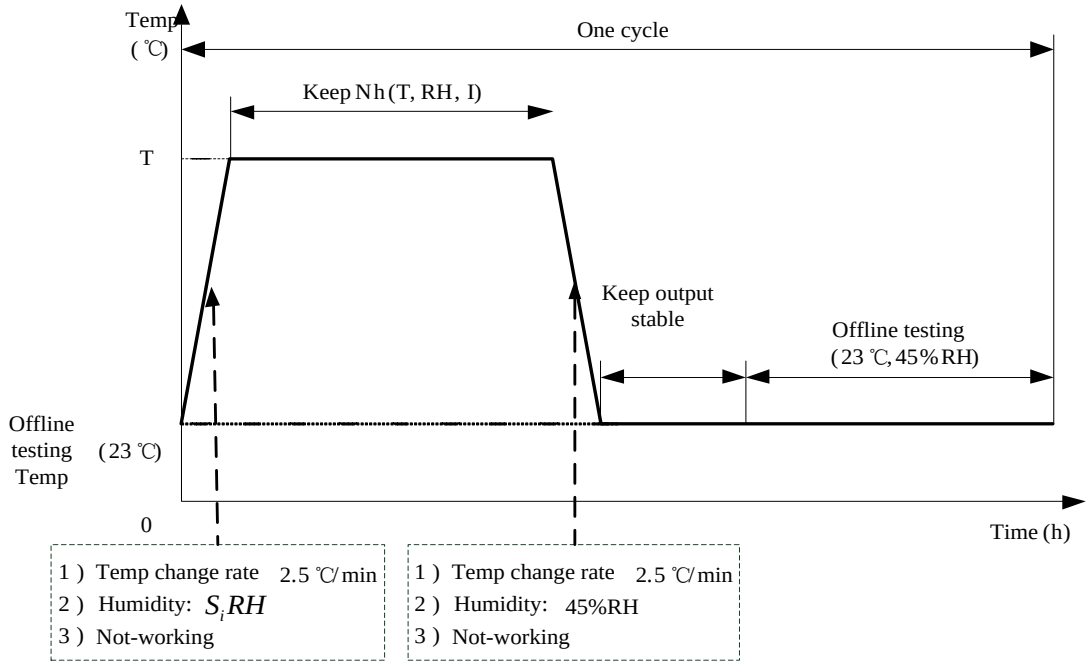


Figure 6. Profile of one testing cycle

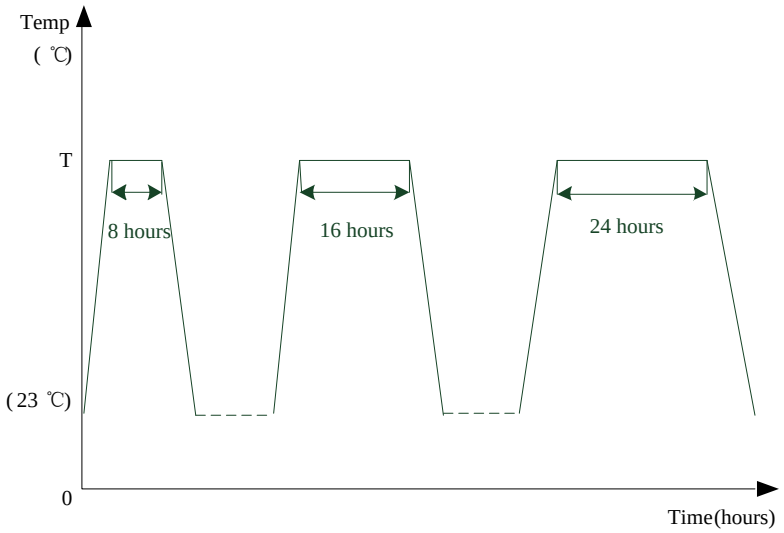


Figure 7. ADT profile

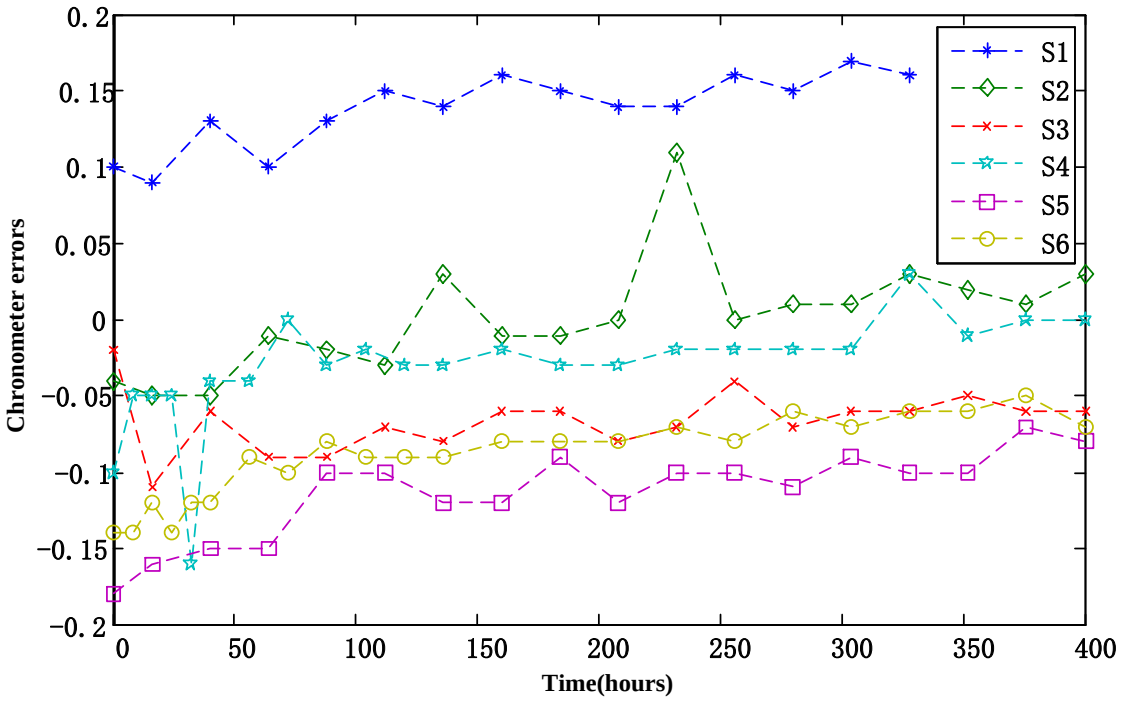


Figure 8. Degradation path of CE of sample No. 5000101 under different designs

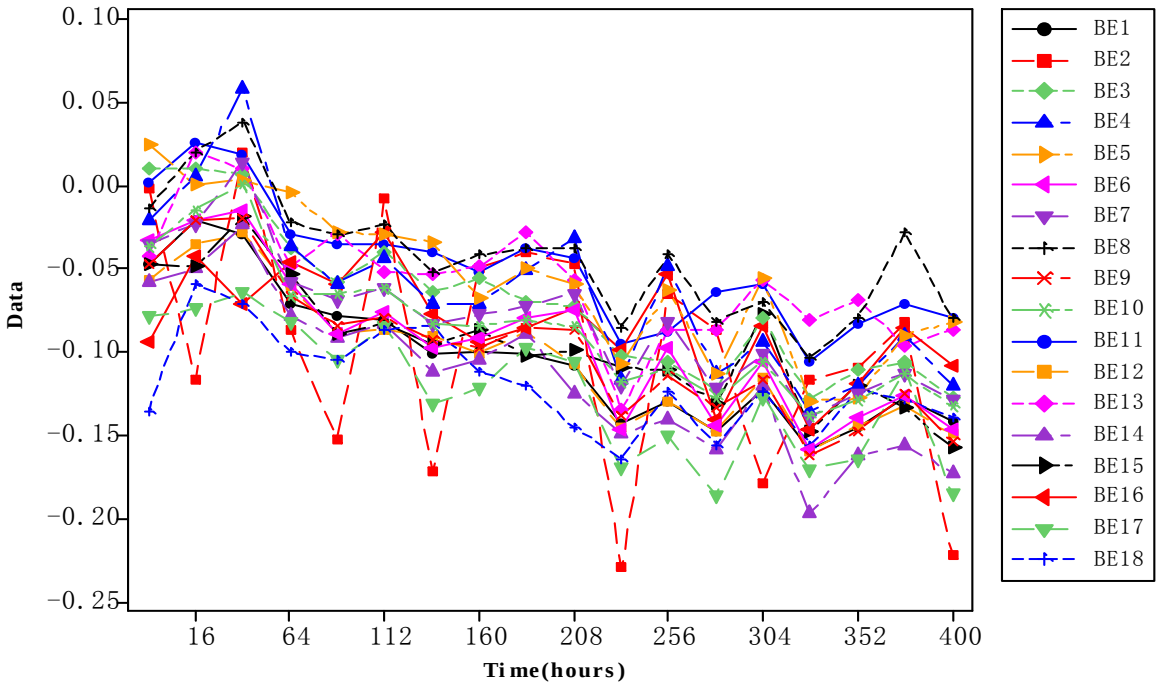


Figure 9. Degradation path of CE of all stresses conditions (sample NO. 5000101)

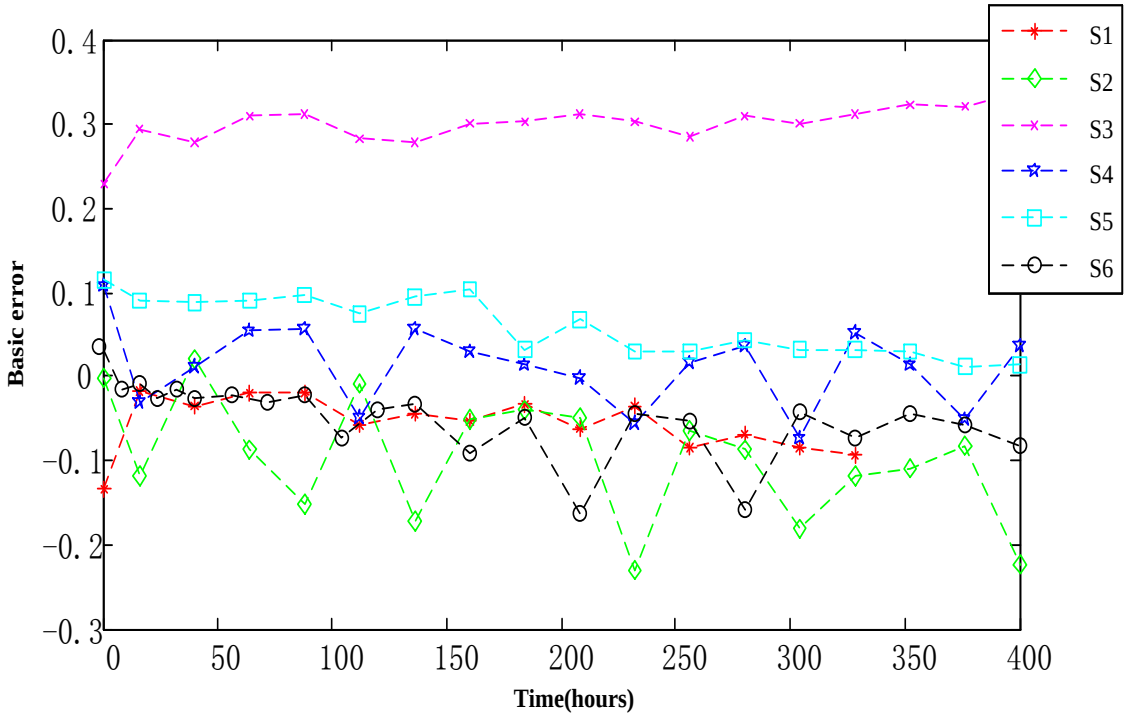


Figure 10. Degradation curves of BE of loading condition No.2 at all stress designs (sample NO. 5000101)

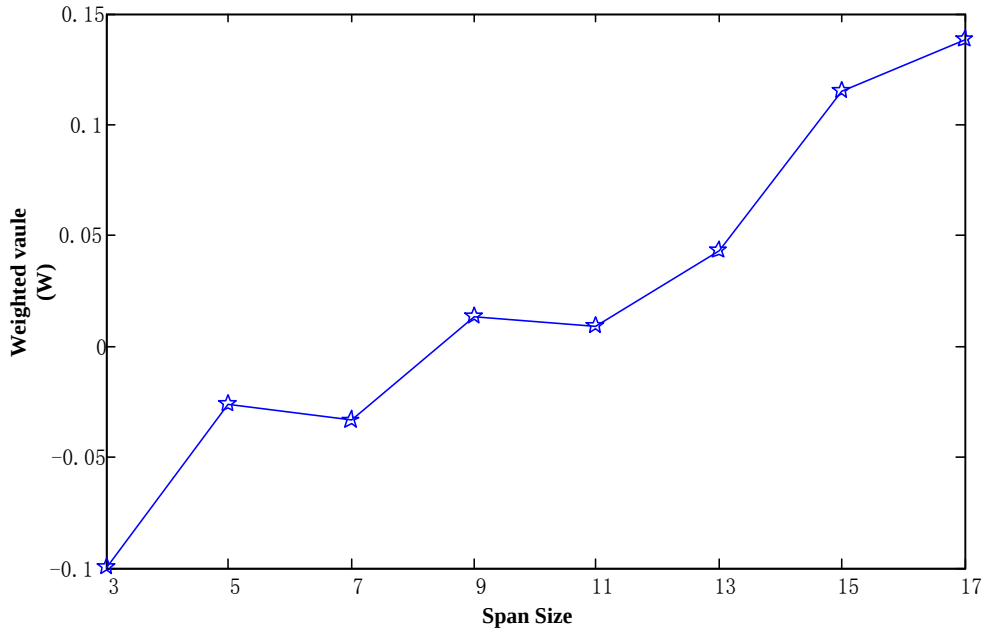


Figure 11. The weighted value of SEM as span size increases (17 is the maximum span size in S2)

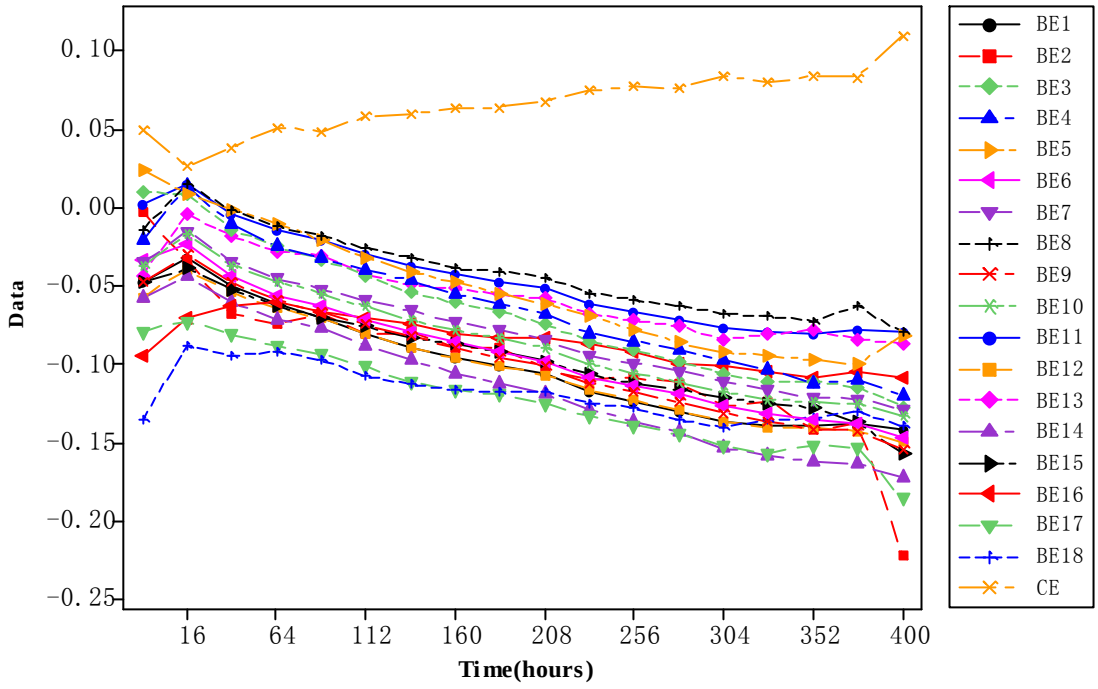


Figure 12. Degradation paths of the sample (No.5000101) after smoothing

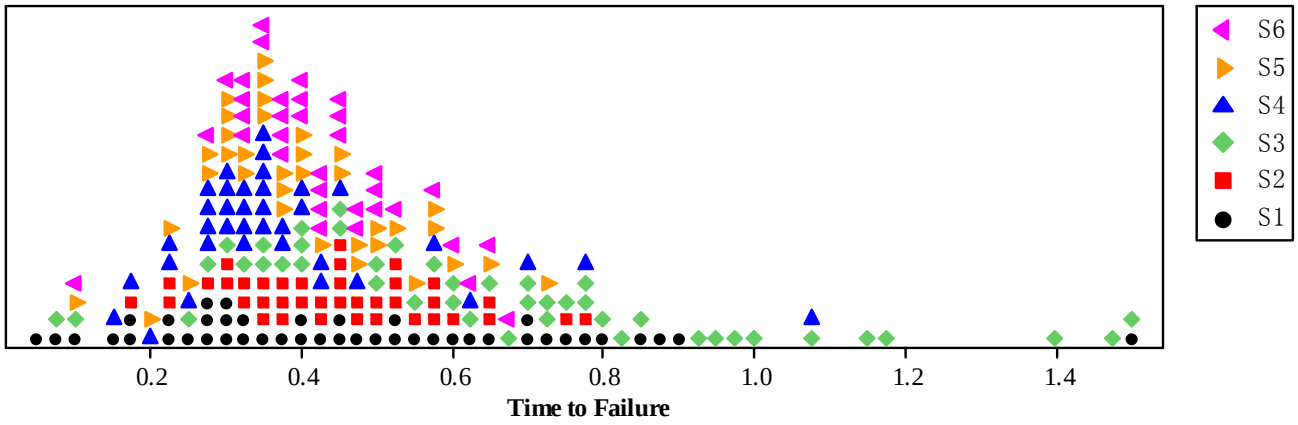


Figure 13. Predicted lifetime of each sample at all stressed conditions

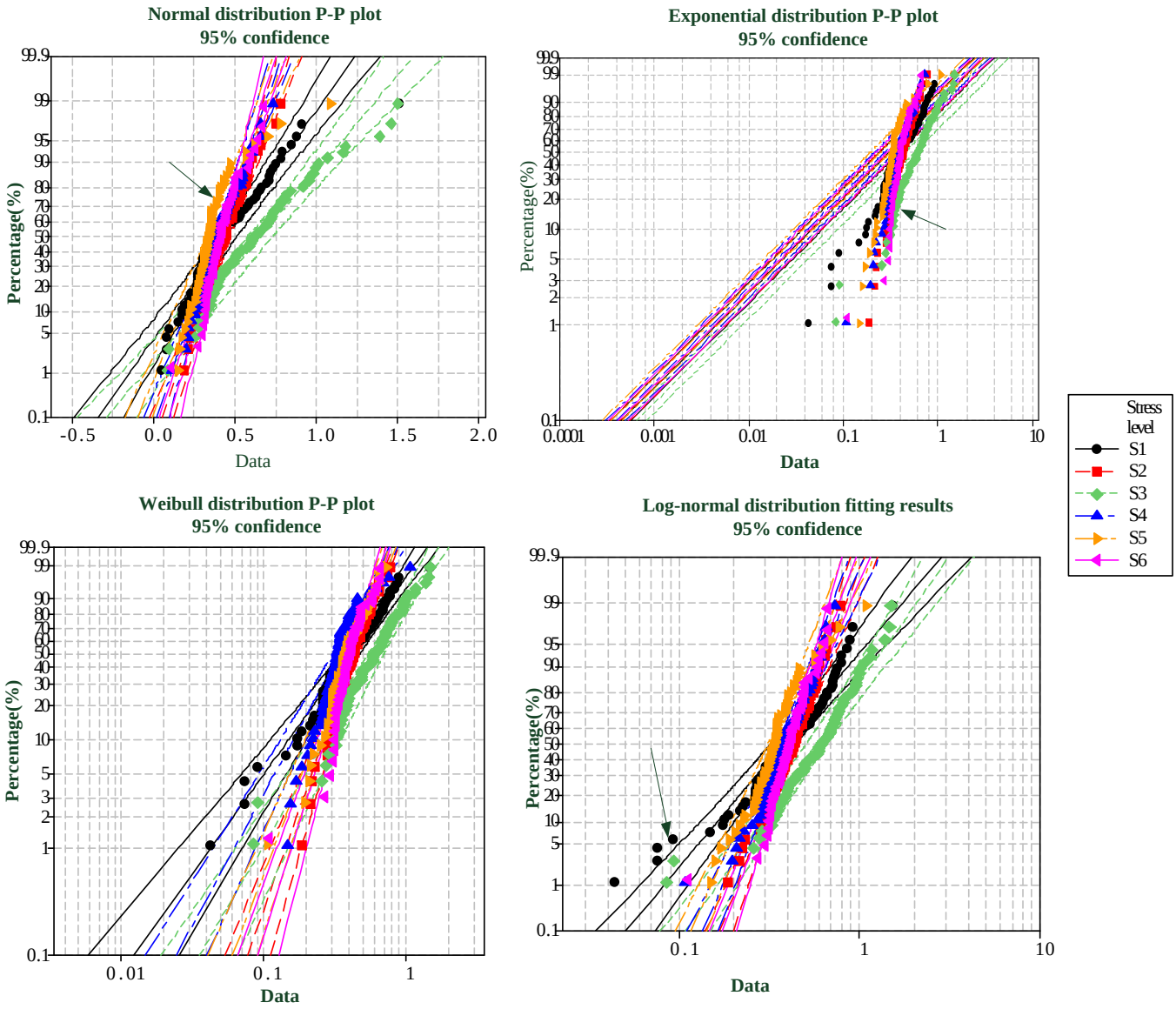


Figure 14. Time-to-Failure data goodness-of-fit of the Weibull distribution

Table I. SEM MODULES AND THEIR FUNCTIONS

| No. | Module | Functions |
|---|---|---|
| 1 | Communication module | Communicating with facilities of electricity stations by sending and receiving data. |
| 2 | Indicating module | Indicating the information of users including electricity consumptions, date, etc. |
| 3 | Power supplying module | Providing the power to SEM via grid power (online) and battery (offline). |
| 4 | Controlling module | Controlling operational status of other modules. |
| 5 | Encrypting module | Encrypting the electricity consumption results. |
| 6 | Billing module | Generating the bills of users and generating warning and refusing signals. |
| 7 | Metering module | Collecting and metering the electricity, isolating the SEM from the main power grid in order to protect the hardware. |
| 8 | Timing module | Providing the reference time to SEM. |

Table II. BILLING-RELATED FAILURE MODES CLASSIFICATION OF IEC62059

| **Criticality** | **Description** |
|---|---|
| Critical failure | A failure affecting billing in anyway (e.g. meter power supply failure, meter out of accuracy class or legal requirements, incorrect time of use or maximum demand computation). |
| Major failure | A failure affecting the collection of the billing data (communications) or the data provided to the final consumer for load management. |
| Minor failure | False alarms, display failure when billing data is collected by other communication means, minor mechanical failure. |

Table III. KEY COMPONENTS OF BILLING-RELATED MODULES AND THE STRESSORS

| **NO.** | **Module** | **Key component** | **Type** | **Stressor** |
|---|---|---|---|---|
| **1** | Metering module | diverter | Resistor | Temperature<br>Humidity<br>Electricity |
| | | Metering chip | Chip | Temperature |
| | | Current transformers | Insulator | Humidity |
| **2** | Controlling module | Controlling Micro Central Unit | Chip | Humidity |

| | | | | |
|---|---|---|---|---|
| **3** | Power supplying module | Isolating transformer | Insulator | Temperature |
| | | Li-battery | Battery | Temperature |
| **4** | Billing module | Billing chip | Chip | Humidity |
| **5** | Timing module | Crystal oscillator | Oscillator | Temperature<br>Humidity<br>Electricity |
| | | Timing chip | Chip | Temperature |

Table VI. SPECIFICATIONS OF THE SEM UNDER TEST

| **Item** | **Value** |
|---|---|
| Current range | 20(80)A |
| Power supply | 230V |
| Frequency | 50Hz |
| Burden: Voltage circuit | <2W and 10VA |
| Burden: Current circuit | <2.5VA at Ib |
| Meter constant | 800 imp /kWh |

Table V. NUMBER OF SAMPLES *n* UNDER DIFFERENT SETTINGS

| $x$ | **0** | | | **1** | | |
|---|---|---|---|---|---|---|
| $\gamma$ / $R$ | 0.7 | 0.8 | 0.9 | 0.7 | 0.8 | 0.9 |
| **0.9** | ≥12 | ≥15 | ≥22 | ≥24 | ≥29 | ≥38 |
| **0.95** | ≥24 | ≥32 | ≥45 | ≥49 | ≥59 | ≥77 |

Table VI. THE DESIGN OF THE SIX EXPERIMENT RUNS

| **NO.** | **Temp (°C)** | **RH (%)** | **I (A)** | **samples** |
|---|---|---|---|---|
| **S1** | 80 | 80 | 20 | 64 |
| **S2** | 80 | 80 | 60 | 64 |

| | | | | |
|---|---|---|---|---|
| **S3** | 55 | 80 | 40 | 64 |
| **S4** | 55 | 95 | 20 | 64 |
| **S5** | 70 | 95 | 60 | 64 |
| **S6** | 70 | 95 | 40 | 56 |

Table VII. THE 18 DIFFERENT LOADS

| NO. | Loading Condition | |
|---|---|---|
| | Current | Power Factor |
| **LC1** | Imax | 1.0 |
| **LC2** | Imax | 0.5L |
| **LC3** | Imax | 0.8C |
| **LC4** | 0.5Imax | 1.0 |
| **LC5** | 0.5Imax | 0.5L |
| **LC6** | 0.5Imax | 0.8C |
| **LC7** | Ib | 1.0 |
| **LC8** | Ib | 0.5L |
| **LC9** | Ib | 0.8C |
| **LC10** | 0.5Ib | 1.0 |
| **LC11** | 0.5Ib | 0.5L |
| **LC12** | 0.5Ib | 0.8C |
| **LC13** | 0.2Ib | 0.5L |
| **LC14** | 0.2Ib | 0.8C |
| **LC15** | 0.1Ib | 1.0 |
| **LC16** | 0.1Ib | 0.5L |
| **LC17** | 0.1Ib | 0.8C |
| **LC18** | 0.05Ib | 1.0 |

* Ib=10A, Imax=60A; C: capacitance loads; L: inductance loads

Table VIII. REGRESSION RESULTS OF THE SAMPLE NO.5000101 UNDER DESIGN LEVEL S2

| Performance indicator | Loading condition | Sum of square for error (SSE) | $R^2$ | slope | intercept |
|---|---|---|---|---|---|
| **BE** | LC1 | 0.009616 | 0.9049 | -0.0471 | -0.0003 |

| | | | | | |
|---|---|---|---|---|---|
| | LC2 | 0.0189931 | 0.6971 | -0.0355 | -0.0003 |
| | LC3 | 0.0094304 | 0.9361 | -0.0044 | -0.0003 |
| | LC4 | 0.0123157 | 0.8901 | -0.0037 | -0.0003 |
| | LC5 | 0.0102741 | 0.8980 | 0.0066 | -0.0003 |
| | LC6 | 0.0081535 | 0.9300 | -0.0362 | -0.0003 |
| | LC7 | 0.0079488 | 0.9345 | -0.0272 | -0.0003 |
| | LC8 | 0.0104789 | 0.8413 | -0.0005 | -0.0002 |
| | LC9 | 0.0070529 | 0.9507 | -0.0408 | -0.0003 |
| | LC10 | 0.0077934 | 0.9353 | -0.0312 | -0.0003 |
| | LC11 | 0.0085557 | 0.8794 | -0.0013 | -0.0002 |
| | LC12 | 0.0082042 | 0.9273 | -0.0488 | -0.0003 |
| | LC13 | 0.0124982 | 0.7042 | -0.0208 | -0.0002 |
| | LC14 | 0.0070861 | 0.9628 | -0.0500 | -0.0003 |
| | LC15 | 0.0076297 | 0.9299 | -0.0454 | -0.0003 |
| | LC16 | 0.0114346 | 0.6005 | -0.0570 | -0.0001 |
| | LC17 | 0.0088175 | 0.8996 | -0.0723 | -0.0003 |
| | LC18 | 0.0136591 | 0.5022 | -0.0942 | -0.0001 |
| **CE** | | 0.0099809 | 0.7334 | 0.0398 | 0.0001 |

Table IX. PARAMETER ESTIMATES OF THE THREE-STRESSORS ACCELERATION MODEL

| **Parameter** | **MLE** | **Fisher matrix** | | | | |
|---|---|---|---|---|---|---|
| | | $\hat{m}$ | $\hat{\alpha}_0$ | $\hat{\alpha}_1$ | $\hat{\alpha}_2$ | $\hat{\alpha}_3$ |
| $\hat{m}$ | 1.7175 | 0.0032 | -0.0269 | 6.8237 | 0.5631 | 0.0003 |
| $\hat{\alpha}_0$ | -14.5267 | -0.0269 | 1.6893 | -449.4764 | -23.1221 | -0.0303 |
| $\hat{\alpha}_1$ | 3184.6269 | 6.8237 | -449.4764 | 139070 | 3037.3073 | 2.2088 |
| $\hat{\alpha}_2$ | 323.9281 | 0.5631 | -23.1221 | 3037.3073 | 1089.5379 | 0.4895 |
| $\hat{\alpha}_3$ | 0.2251 | 0.0003 | -0.0303 | 2.2088 | 0.4895 | 0.0051 |

Table X. PREDICTED LIFETIME OF ALL THE SAMPLES AT TWO PAIRED DESIGN LEVELS

| **Design pairs** | **Samples** | **Wilcoxon signed** | **P-value** | **Estimated median** |
|---|---|---|---|---|

| | rank | | | |
|---|---|---|---|---|
| **S1-S2** | 64 | 1027.0 | 0.933 | -0.002202 |
| **S5-S6** | 56 | 647.0 | 0.220 | -0.02976 |

Table XI. PARAMETER ESTIMATION OF TWO-STRESSORS ACCELERATED MODEL

| **Parameter** | **MLE** | **Fisher Matrix** | | | |
|---|---|---|---|---|---|
| | | $\hat{m}$ | $\hat{\alpha}_0$ | $\hat{\alpha}_1$ | $\hat{\alpha}_2$ |
| $\hat{\mathbf{m}}$ | 1.6912 | 0.0031 | -0.0255 | 7.0737 | 0.4699 |
| $\hat{\alpha}_0$ | -13.005 | -0.0255 | 1.5268 | -452.0283 | -17.8092 |
| $\hat{\alpha}_1$ | 3032.0397 | 7.0737 | -452.0283 | 1.47E+05 | 2026.3353 |
| $\hat{\alpha}_2$ | 301.0359 | 0.4699 | -17.8092 | 2026.3353 | 1036.9996 |

Table XII. Reliable lifetime $t_\gamma$ of SEM

| **Temperature** | **Confidence** / **Reliability** | **0.7** | **0.8** | **0.9** |
|---|---|---|---|---|
| **20℃** | 0.9 | 11.8434 | 10.2991 | 8.485 |
| | 0.95 | 7.7109 | 6.6912 | 5.4963 |
| **25℃** | 0.9 | 10.0212 | 8.7493 | 7.248 |
| | 0.95 | 6.5247 | 5.6845 | 4.6952 |